Fabrication and Characterization of Nano-engineered Membranes for Oil-Water Separation

by

Brian R. Solomon

B.S.E., Mechanical Engineering
Duke University (2011)

Submitted to the Department of Mechanical Engineering
in partial fulfillment of the requirements for the degree of

Master of Science in Mechanical Engineering

at the

MASSACHUSETTS INSTITUTE OF TECHNOLOGY

June 2013

Author .....
Department of Mechanical Engineering
May 10, 2013

Certified by .....
Kripa K. Varanasi
Doherty Chair in Ocean Utilization
Associate Professor of Mechanical Engineering
Thesis Supervisor

Accepted by .....
David E. Hardt
Ralph E. and Eloise F. Cross Professor of Mechanical Engineering
Chairman, Department Graduate Committee

Fabrication and Characterization of Nano-engineered Membranes for Oil-Water Separation

by

Brian R. Solomon

Submitted to the Department of Mechanical Engineering
on May 10, 2013, in partial fulfillment of the
requirements for the degree of
Master of Science in Mechanical Engineering

Abstract

The focus of this thesis is the design and testing of membranes for separation of water-in-oil (w/o) emulsions. A polycarbonate membrane treated with octadecyltrichlorosilane (OTS) is used to filter a 3 wt% w/o emulsion. The permeate is characterized to have no measurable water content by microscopy, dynamic light scattering (DLS) and differential scanning calorimetry (DSC). To extend this work, a method for fabricating an asymmetric polysulfone membranes is presented. The polysulfone membrane has the feature of allowing much higher flow rates for a given applied pressure.

The research is largely motivated by a need for low cost methods for separating o/w and w/o emulsions. The largest source of wastewater is generated by the petroleum industry as o/w emulsions. Currently, industry has a number of methods for cleaning produced water. The inherent problem is that the smaller dispersed droplets are the more expensive they are to separate.

In addition, the fundamental equations and models that govern interfacial phenomena and hydrophobic/oleophilic membranes are developed. In all, this work present a method for successfully separating oil droplets smaller than a micron from water by a novel methodology.

Thesis Supervisor: Kripa K. Varanasi
Title: Doherty Chair in Ocean Utilization
Associate Professor of Mechanical Engineering

Acknowledgements

To start, I thank my mother. Simply put, I would not be here without her.

I thank my advisor Professor Kripa Varanasi. I am grateful for his motivation, creativity, and most of all his patience. Also, I thank Nasim Hyder who collaborated with me on many aspects of this project. I also give thanks to the Mechanical Engineering Department here at MIT as well as the Laboratory for Manufacturing Productivity.

I thank other members of my lab - Dave, Adam, and Chris for inspiring me and being my role models. Seyed for keeping me entertained and my mind racing. Karim and Srinivas for working with me last minute on those problem sets. And to Sushant, Hyuk-Min, Giselle, Divya, Yuehua, Rajeev, Nada, Alex, Konrad, Navdeep and Lauren for the countless discussions and support.

I thank my dance coach Armin Kappacher. As Armin says, dancing is life. And thanks to the other great teachers I've had in my life of which there are too many to name.

I thank the MIT Energy Initiative and Shell for the fellowship funding they have awarded me.

I started to write out names of close friends who I wanted to thank, but twenty names into it I realize there are too many to fit on this page. You guys know who you are. To everyone who has had a part in my life especially in these past two years - thank you all!

Contents

List of Figures

Abbreviations and Symbols

Γ	adsorption
μ	chemical potential
μ	dynamic viscosity
ρ	density
g	acceleration due to gravity
N^{σ}	surface excess number of molecules
S^{σ}	surface excess entropy
U^{σ}	surface excess internal energy
V_m	molar volume
API	American Petroleum Institute
c	molality
DAF	dissolved air flotation
ESEM	environmental scanning electron microscope
γ	surface tension or interfacial tension
θ	contact angle
A	cross-sectional area

k	permeability
L	thickness
P_B	breakthrough pressure
r_p	pore radius
AB	Lewis acid/base
IAF	induced air flotation
BOD	biochemical oxygen demand
DO	dissolved oxygen
DSC	differential scanning calorimetry
LW	Lifshitz-van der Waals
MF	microfiltration
o/w	oil in water
OTS	octadecyltrichlorosilane
PEG	polyethylene glycol
ppm	parts per million
Q	volumetric flowrate
UF	ultrafiltration
w/o	water in oil
Psf	polysulfone
x	molecular concentration

Chapter 1

Introduction

Over the past few decades, membrane technologies for particle separation have advanced substantially. Membranes have found use in catalytic reactors,[2] protein purification,[3] and gas separation.[4]

The science governing the wetting of liquids, more broadly referred to as interfacial science, has also advanced a lot over the past decade. Many are familiar with the "lotus effect" that allows a lotus leaf to repel water.[5] Wilhelm Barthlott of the Univeristy of Bonn in Germany is largely credited with the discovery of the lotus effect. The sacred lotus (*Nelumbo nucifera*) is an aquatic perennial that grows in muddy waters. Despite living among dirty conditions, the leaves are always clean. Drops of water on a lotus leaves rolls off easy, and the surface is the classical example of a superhydrophobic surface.

The discovery of the lotus effect sparked a revitalization in interfacial science and has since led to surfaces that are super-slippery,[6] anti-fogging[7] and self-cleaning.[8]

The goal of this work is to design membranes that can separate water-in-oil (w/o) emulsions based on the difference in their respective interfacial tensions. The fundamentals governing such a system are explored, and results of testing membranes are presented. In addition, current industrial methods for oil-water separation are reviewed.

As the forthcoming work shows, the principles governing the separation of w/o emulsions also holds for oil-in-water (o/w) and more generally any two phase system. Accordingly, the work applies more broadly to many multiphase systems in which separation is desirable.

Figure 1.1: Water rolling off a lotus leaf demonstrating the lotus effect.[1]

1.1 Motivation

1.1.1 Oil-Water Separation

Impure water generated during crude oil and natural gas recovery and production is referred to as produced water. Produced water is the single largest volume of waste generated in the oil and gas industry. During later stages of oil production, up to 98% of the fluid extracted from reservoirs is produced water. Produced water is characterized by a continuous water phase with dispersed oils, solids, and other contaminants. This emulsion can occur naturally in the reservoir or result from the extraction process as fluid is brought up through wellhead chokes, various pipes, headers, control valves and pumps.[9]

The need to purify produced water is dictated by governmental regulation. The Clean Water Act establishes a comprehensive program to restore and maintain the chemical, physical, and biological integrity of national waters.[10] Typical regulations prohibit the discharge of wastewaters in which the oil content is greater than 10-15 ppm.[11] Industrially deployed separation systems usually comprise a primary, secondary and if necessary tertiary treatment phase for the removal of oils.[12] Primary treatment involves techniques that leverage the density difference between oil and water and are effective for removing free oils (diameters larger than 150 μm).

Oil content in produced water is regulated because organics discharged to the environment has detrimental effects on the system's ecology. With an organic material, the amount that can be safely absorbed by the received body of water is defined by its effect on he dissolved oxygen (DO) level in the water. The saturation value of DO is 8-15 mg/L depending on temperature and salinity of the water. Organisms that consume the organic matter consume oxygen in the process starve oxygen from other organisms that require it. The biochemical oxygen demand (BOD) is the amount of oxygen microorganisms require to oxidize organic wastes aerobically over a specific amount of time at a specific temperature and has been the most important measure of strength of organic pollution. The most common measure of BOD is the total amount of oxygen per liter consumed by the microorganisms during the first five days of biodegradation at 20°C.[12]

In addition to oil-in-water emulsions, water-in-oil emulsions are of concern in the petroleum industry. About 80% of the worlds crude oil exists in a water-in-oil emulsion.[13] It is costly to transport crude oil with such high water contents. In addition, salts present in the water contribute to fouling and corrosion of processing equipment. Water is also intentionally dispersed into the crude oil to dissolve hydrophilic constituents during refining.[14] Such water must subsequently be removed.

The most common way of removing wash water that was introduced to dissolve salts is by electrocoalesence. In electrocoalescence an electric field is applied usually with voltages on the order of kilovolts to cause polarization of water droplets. The water droplets then attract each other and coalesce. Electrocoalescence systems must be finely tuned based on the dielectric properties of the oil phase as well as the amount of water present.[15] As a result, a large amount of technological support is required to keep systems running. A membrane system is more widely applicability.

1.1.2 Abstraction to Other Systems

While this work focuses on oil-water systems, it can be extended to any multiphase system. Essentially, the difference in surface tension between water and oil is leveraged in the separation process used in this work. Any other immiscible substances can be separated

this way.

One major industry that makes use of emulsions is food processing. Milk for example contains many emulsified compounds where their separation is useful to sell them separately. In pharmaceutics, emulsions a frequently used for the transport of drugs.

Chapter 2

Review of Industrial Methods

Oily wastewater is generated in many industries including petroleum refining, petrochemicals, food, leather finishing and metal finishing.[12] Current treatments consist of a series of treatments to bring oil concentrations to desired levels. These treatments are grouped into primary, secondary and tertiary treatments.

2.1 Primary Treatments

Primary treatments leverage the difference in density between water, oil and solids. Essentially solids and oils heavier than water will sink out of the mixture and phases lighter than water will float up.

The settling or rising of a particle due to buoyancy can be expressed by Stokes' law. For a solid particle experiencing a buoyancy force due to gravity in water, the terminal velocity it reaches is:

$$v_s = \frac{2}{9}\frac{\rho_p - \rho_w}{\mu} g R^2 \tag{2.1}$$

As evident, the smaller a particle or droplet the lower its terminal velocity. As a result, small droplets and particles will take significantly longer than their larger counterparts. Additionally, for particles with small terminal velocities convectional currents and thermal fluctuations in the continuous phase is enough to prevent the particles from ever settling or

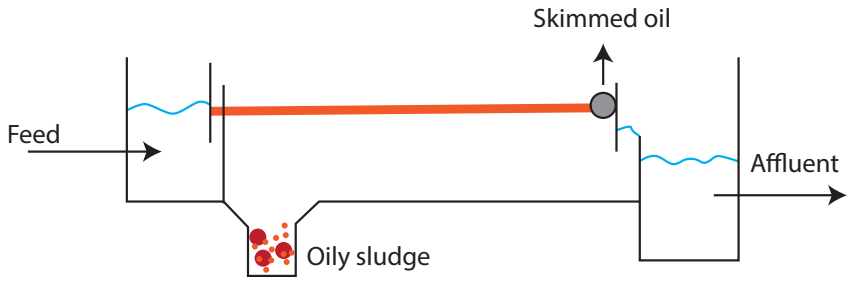

Figure 2.1: Diagram of a typical API separator.

rising out of the continuous phase.

As a result, primary treatments can only separate droplets larger than about 30 μm or so. For separating smaller droplets, secondary and tertiary treatments must be used.

2.1.1 API Separators

In the petroleum refining industry API separator design is specified by the American Petroleum Institute (API). Figure 2.1 is a schematic of a typical API separator. The system consists of a tank with a surface skimmer and bottom rake to remove floating oil and solids respectively. The system works best on free oil larger than 150 m. Water is continuously fed in and the parameters of the system must be matched such that there is enough time for droplets and solids to float or fall out. Effluent leaving a separator usually has oil droplets smaller than 30 m and oil concentrations less than 200 mg/L.[12]

2.1.2 Plate Coalescers

One extension of the API separator that is now readily employed is the plate coaslecer. Rather than flow freely through the API separator, water is passed through a series of parallel plates. Oil droplets rise and stick to the plates and coalesce with other oil droplets. Once they reach a critical size, the drops then float to the top and are skimmed off. Effectively the distance a rising oil droplet must cover is reduced.

The plates are often made of oleophilic polypropylene. Plate coalescers require less space than conventional API separations and can removal virtually all droplets larger than 20 μm. The drawback is that the plates can become clogged with solids.[16]

2.1.3 Centrifuges

Centrifugation is an efficient method of separating emulsions as is often used in small workshops and labs. The general principal is to spin an emulsion. Oil drops will experience a centrifugal force outwards and separate out quicker than they otherwise would by gravity.[17] Still, the terminal velocity is limited as predicted by Stokes' law. Centrifugation effectively increases the gravitational acceleration in Equation 2.1.1.

Several different form factors can be used including tubular, disk-stack[18] and hydrocyclones. Hydrocyclones are a particular class of centrifuges where the liquid feed is forced into a circular motion. They have the advantage of being able to continuously processes feed.

2.2 Secondary Treatments

Secondary treatments consist of chemical, physical and electrical methods. Almost always some sort of chemical demulsifier is employed in their operation.

2.2.1 Chemical

Oil droplets are in part stabilized by electrostatics. Chemical additives can destabilize the dispersed phase by reducing their surface charge.

The addition of coagulants (inorganic salts) increases the conductivity of the continuous face and reduces the effective width of the electric double layer around oil droplets. Accordingly, the zeta potential is reduced and droplets are able to aggregate.

Polyelectrolytes and organic polymers can also be employed to change the surface charge of droplets or form bridges by polymerization. In these techniques, further processing (including previously mentioned techniques) must be used to separate the now coagulated droplets.

2.2.2 Flotation

Flotation is a process by which air is introduced to the wastewater stream. Air tends to stick to oil droplets and will lift them up by buoyancy.[19,20] This is accomplished because air is significantly less dense that oil.

The two types of commercial flotation processes are induced air flotation (IAF) and dissolved air flotation. The fundamental difference is the IAF uses impellers to introduced bubbles into the stream where DAF directly injects air to create bubbles.

2.2.3 Filtration

Filtration has been employed in a number of methods. One such is deep-bed filtration where the emulsion passes through a packed bed that either absorbs oil or promotes droplet coalescence. In addition, membrane systems similar to ones in this work are used. The difference is that currently used membrane are not chemically altered to leverage differences in phase surface tension. Current membranes treat emulsion separation as similar to particle separation. As shown later, this is not the case. It should be noted that any filtration system tends to decrease in performance over time due to accumulation of solids that increase the pressure drop needed to maintain flow.

2.3 Tertiary Treatments

Tertiary treatments are used as the last line to remove oil from wastewater. These methods are less cost effective, so processes earlier in the chain are used to remove as much oil as possible.

One method is evaporation. Evaporation requires a large amount of energy. There are several types of evaporators commercially used. The dynamics of evaporation is explained by a three step process. First, water transports to the top of the evaporation column, then transports through the thin layer of oil and finally evaporates.

Repulsive forces between oil droplets tend to decrease the vapor pressure and thus increase the energy needed for evaporation. Additionally, evaporators do not remove oils

but instead remove water. They are labor intensive and thus not often suited for large scale processing.

Another technique is active carbon adsorption. Active carbon adsorption is based on the use of an activated carbon bed. The process requires the activated carbon to be reactivated. Both the activated carbon and its reactivation is expensive.[21] In addition, biological treatments and reverses osmosis are also used but both have inherent drawbacks. Biological treatment is very sensitive to the parameters of the system. Reverse osmosis suffers from membrane fouling and can support only very small flow rates.

As a final step in obtaining pure water, these techniques are employed when certain purities are desired. Oftentimes required purities can be achieved by secondary treatments or sometimes just primary treatments depending on the feed.

Chapter 3

Fundamentals of Interfacial Science

Interfacial is an interdisciplinary field combining chemistry, physics, nanotechnology and other fields. Understanding of interfacial phenomena can answer questions such as how can bugs walk on water?[22] What determines the size distribution of raindrops?[23]

Answers to these questions lie in the fundamentals of what governs interactions at interfaces. Four canonical equations in the field of interfacial science are the Young-Laplace Equation, Young's Equation, the Gibbs Adsorption Equation and the Kelvin Equation. Together, they form the basis for phenomena arising at and as a result of interfaces.

3.1 Four Fundamental Equations of Interfacial Science

3.1.1 The Young-Laplace Equation

The Young-Laplace equation relates the pressure difference across a curved surface of two static phases.

$$\Delta P = \left(\frac{1}{R_1} + \frac{1}{R_2} \right) \tag{3.1}$$

In this equation R_1 and R_2 are the radii of curvature. A simple derivation is presented here, but more complicated derivations can be found in many canonical textbooks.[24,25]

To start, consider figure Figure 3.1. A spherical cap is allowed to deform by applying

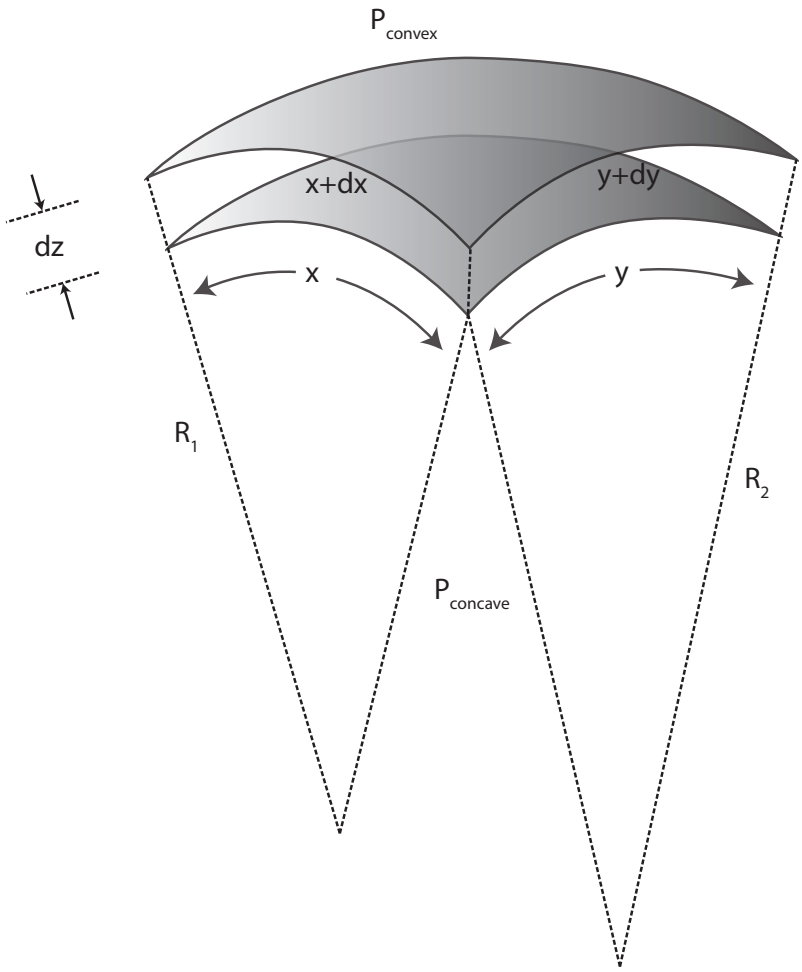

Figure 3.1: Deformation of a spherical cap under a pressure difference.

a pressure difference from the concave to the convex side. The pressure work required to deform the surface can be written as:

$$W = \Delta PV = \Delta P \mathrm{d}z A = \Delta P x y \mathrm{d}z \tag{3.2}$$

The total energy of the surface is the surface's surface tension multiplied by its area. Therefor, the work can also be expressed as the differential energy of the surface written in terms of the differential area.

$$W = \gamma \mathrm{d}A = \gamma(x\mathrm{d}y + y\mathrm{d}x) \tag{3.3}$$

Setting these two works equal yields:

$$\Delta P x y \mathrm{d}z = \gamma(x\mathrm{d}y + y\mathrm{d}x) \tag{3.4}$$

$$\Delta P = \gamma\left(\frac{1}{x}\frac{dx}{dz} + \frac{1}{y}\frac{dy}{dz}\right) \tag{3.5}$$

It can be shown by observing the similar triangles of the system that this equation reduces to:

$$\Delta P = \gamma\left(\frac{1}{R_1} + \frac{1}{R_2}\right) \tag{3.6}$$

Though not presented here, the derivation can also be carried out for an arbitrary surface deforming under an pressure difference. For such a case Equation 3.6 also holds where the radii of curvature can be determined by considering differential geometry.

Equation 3.6 states that there is necessarily a pressure drop across a curved surface that is related to its surface tension. One interesting situation is a surface that has two radii of curvature that are equal but opposite. In such a case, there will be no pressure difference despite a curved surface.

The Young-Laplace equation explains a simple experiment. Take a glass slide and place a water drop on it. Then place another glass slide on top. One will find it nearly impossible to pull the two glass slides apart. Essentially, the water between the slides has a very small radius of curvature. Equation 3.6 predicts a very high suction pressure inside the water film that pulls the glass slides together.

3.1.2 Young's Equation

Young's Equation relates the contact angle of a droplet of liquid on a surface to the surfaces energies of the phases present.

$$\gamma_{LV}\cos\theta = \gamma_{SV} - \gamma_{SL} \tag{3.7}$$

By observing Figure 3.2, the derivation is evident from a force balance of the horizontal

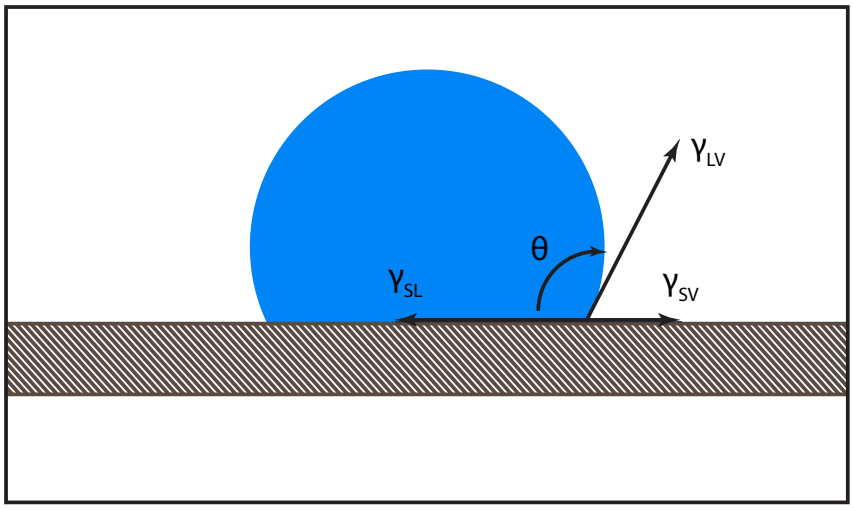

Figure 3.2: A spherical droplet resting on a substrate. The force arising from the three surface tensions are balanced in the horizontal direction.

surface tension components. While simple to derive, there a a few subtleties of the equation that must be discussed.

To start, there is almost never just one contact angle observed. More often, when an interface is advancing the contact angle takes on a larger value than when the interface is receding. These contact angles are referred to as the advancing and receding contact angles, and their difference is known as contact angle hysteresis.

Surfaces with both low and high (greater than 50°) differences have been reported. Hystersis is an important factor in determining drop rolloff. Paxson et. al visualized moving droplets in an environmental scanning electron microscope (ESEM) and observed the nature of contact angle hysteresis.[26]

3.1.3 The Gibbs Adsorption Equation

The Gibbs Adoprtion Eqution relates the change in surface tension of an interface to the adsorption of components to the interface. There are many assumptions in arriving at such an equation, and one form of the equation is:

$$-\mathrm{d}\gamma = RT\Gamma\mathrm{d}(\ln c) \tag{3.8}$$

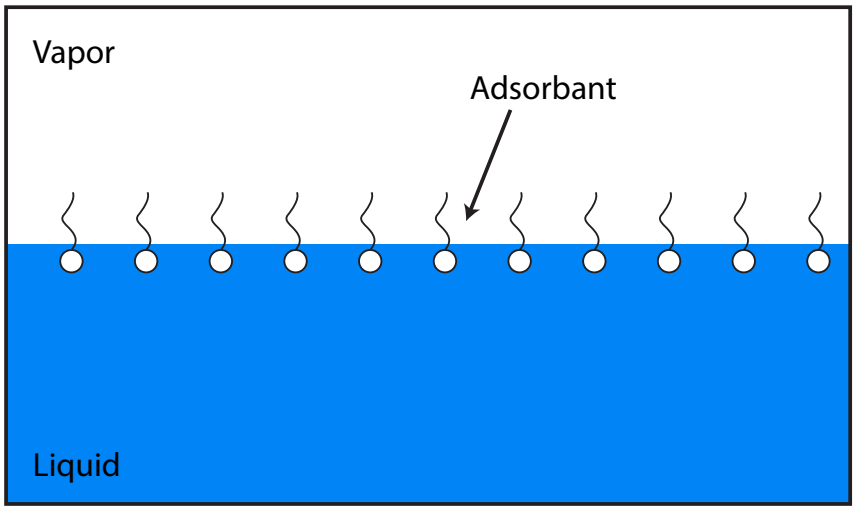

Figure 3.3: Components adsorbing to the vapor/liquid interface.

Figure 3.3 shows the situation this equation describes. Adsorbants (either from the gas or dissolved in the liquid) will absorb to an interface and lower its surface tension. Note that the adsorption need not be positive. Salts in water for example will have a negative adsorption and lead to increased surface tension.

To understand the limitations of the above equation. A derivation is presented here. Consider an interface described by the Gibbs dividing surface. The differential internal energy can be written as:

$$\mathrm{d}\underline{\mathrm{U}}^{\sigma} = T\mathrm{d}\underline{\mathrm{S}}^{\sigma} + \sum_{j=1}^{n} \mu_j \mathrm{d}N_j^{\sigma} + \gamma \mathrm{d}\underline{\mathrm{A}} \tag{3.9}$$

Here an under bar denotes an external variable of the system, and the σ superscript denotes a quantity of the dividing surface. By integrating the Equation 3.9, differentiating it again and subtracting from Equation 3.9:

$$-\gamma \mathrm{d}\underline{\mathrm{A}} = \underline{\mathrm{S}}^{\sigma}\mathrm{d}T + \sum_{j=1}^{n} N_j^{\sigma}\mathrm{d}\mu_j \tag{3.10}$$

Now the adsorption can be defined and the Gibbs Adsoprtion Equation for a flat inter-

face is found to depend on the adsorption of the components of the system.

$$\Gamma_j = \frac{N_j^\sigma}{\underline{\mathrm{A}}} \tag{3.11}$$

$$-\gamma = S^\sigma \mathrm{d}T + \sum_{j=1}^{n} \Gamma_j \mathrm{d}\mu_j \tag{3.12}$$

The entropy expressed in this equation is no longer taken to be extensive as the equation has been divided through by the specific area. To proceed, consider a system at a constant temperature, so the entropy component drops out. In addition, a model of the chemical potential of the components must be assumed. For simplicity, consider only one component adsorbing to the surface. For an ideal solution the chemical potential of a component is:

$$\mu_j(T,P,x_j) = \mu_i^0(T,P) + RT \ln x_j \tag{3.13}$$

The term μ_i^0 is only weakly dependent on pressure, so for constant temperature:

$$\mathrm{d}\mu_j(T,P,x_j)|_{t=0} = RT\,\mathrm{d}\ln x_j \tag{3.14}$$

For dilute solutions, the molecular concentration is equal to the molarity. Thus by plugging Equation 3.14 into Equation 3.12 the Gibbs Adsorption Equation of Equation 3.8 is recovered.

3.1.4 The Kelvin Equation

The Kelvin Equation relates the actual vapor pressure to the saturated vapor pressure as a function of the radius of a droplet. It can be written:

$$\ln\left(\frac{P}{P_0}\right) = \frac{2\gamma V_m}{rRT} \tag{3.15}$$

To begin, consider the situation of Figure 3.4. A liquid droplet sits in equilibrium with

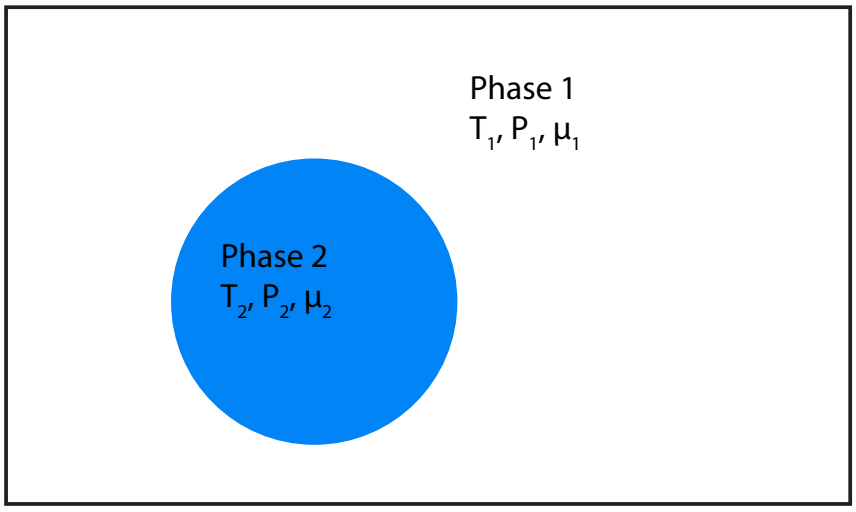

Figure 3.4: A liquid droplet in the presence of its own vapor.

its vapor. The Gibbs-Duhem equation can be written for both of the two phases present:

$$S^V \mathrm{d}T - V^V \mathrm{P} + \mathrm{d}\mu = 0 \tag{3.16}$$

$$S^L \mathrm{d}T - V^L \mathrm{P} + \mathrm{d}\mu = 0 \tag{3.17}$$

Now, several assumptions are made. The first is that the liquid is incompressible. It is also assumed that there is much more vapor present than liquid (i.e. $V^V >> V^L$). Finally, it is assumed that the vapor follows the ideal gas law. By writing the Equation 3.1 for the two phases and making use of the assumptions, one can write:

$$\mathrm{d}\left(\frac{2\gamma}{r}\right) = \frac{RT}{V^L}\mathrm{d}\ln P^V \tag{3.18}$$

Integrating yields Equation 3.15 as desired. It is important to notice the implications of this result. The equilibrium vapor pressure depends on droplet size. This explains the phenomena of superheating and supercooling.

3.2 Emulsions and Factors Affecting Their Stability

Crude oil contains naturally occurring compounds that contribute significantly to the stability of emulsions arising from them. These compounds include asphaltenes, resins, calcite, silica and microcrystalline waxes, and their composition in various crude oils varies among recovery sites drastically.[27] Water-in-crude oil emulsions are most stable for a particular ratio of such compounds. Mohammed et al. found that a 1:1 resin to asphaltenes resulted in the most stable interfacial film.[28] It has also been found that the temperature history of the crude oil affects the stability of the proceeding emulsions. For example, the cooling rate determines the crystal structure of precipitated waxes (whether finely dispersed or aggregate) that in turn contribute to interfacial film stability differently.[29]

These compounds increase the stability of emulsions by two separate mechanisms. First, many of these compounds act as surfactants and lower the interfacial tension of the oil/water interface. This lowers the total energy of the dispersed system and thus increases its stability.

In addition, particles absorbed at the interface form rigid films that prevent drops from coalescing. The pure example of this is a Pickering emulsion. Vignati et al. studied a simple system of oil-in-water stabilized by silica particles. Remarkably, the emulsion was extremely stable despite having the same interfacial tension as that of a pure oil/water system.[30] Due to the complex dynamics introduced by many components of naturally occurring emulsions, a system consisting of only pure water, pure hexadecane and a non-ionic surfactant (Span 80) is considered in this work.

Causing an emulsion to resolve to its component phases is referred to as breaking the emulsion. Treatments to break emulsions consist of chemical, physical and electric methods include filtration. Microfiltration (MF) describes systems in which the pore size ranges from 10 μm to 100 nm, whereas ultrafiltration (UF) refers to pore sizes from 100 to 1 nm.[31] Traditionally, the hydrophilicity of MF and UF membranes have been studied in great depth for influencing the permeate flux.[32–34] Such membranes are employed for filtration of non-deformable components such as protein aggregates and macromolecules. In such a case, the minimum pore size necessarily restricts any particles larger from permeat-

ing in the membrane. In filtration of emulsified liquids however, the dispersed droplets are capable of deforming and squeezing through smaller pores.[35,36] This begs the question of what variables must be considered for designing a system to separate emulsified liquids.

Chapter 4

Membrane Design

Recently, specially coated membranes have been used for separation of o/w and w/o emulsions.[37–39] These membranes demonstrate successful and complete separation of emulsions with the transmembrane pressure being applied via the hydrodynamic head of the emulsion.

In such studies, gravity fed separation was successfully achieved for droplets larger than about 20 μm at best. Rejection of these large droplets can be achieved by relatively large pore sizes. The pressure needed to achieve adequate permeate flux through such large pores need only be provided by a hydrodynamic head.

While able to separate large droplets, large size membranes offer no separation of very small droplets. Intuitively, decreasing the pore size of the membrane allows for the rejection of smaller droplets. For a fixed pressure, the flow rate scales inversely with the fourth power of the radius of the pores as dictated by Hagen-Poiseuille flow. While with larger pore sizes a transmembrane pressure supplied by only hydrodynamic head can offer reasonable flow rates, at smaller pore sizes gravity fed filtration is ineffectively in achieving satisfactory flow rates.

4.1 Design Approach

Accordingly, its important to understand not only a membranes affinity for water (hydrophobicity) but also its affinity for oils (oleophilicity). In general, a liquid is said to

wet a solid surface if it exhibits a contact angle less than 90°. For a liquid L and apolar solid S, the contact angle θ_C is given by a modified version of Youngs equation.[40]

$$\gamma_S = \frac{\gamma_L(1+\cos\theta_C)^2}{4} \tag{4.1}$$

Accordingly for a given apolar solid surface as a liquid's surface tension decreases so does its contact angle. In the case of water ($\gamma = 72$ dyn/cm) and oil ($\gamma \approx 22$ dyn/cm), a given apolar membrane will always be more oleophilic than hydrophilic. Such membranes can theoretically reject all emulsified water droplets above its minimum pore size given appropriate operating conditions but will be unable to completely reject emulsified oil droplets.

Recently, coatings have been developed that are more wetting to water than oil.[41,42] Such behavior can be attributed to polar interactions between the membrane surface and water and can be expressed in terms of Lifshitz-van der Waals (LW) and Lewis acid/base (AB) interactions.[43]

$$\gamma_L(1+\cos\theta_C) = 2(\sqrt{\gamma_S^{LW}\gamma_L^{LW}} + \sqrt{\gamma_S^{+}\gamma_L^{-}} + \sqrt{\gamma_S^{-}\gamma_L^{+}}) \tag{4.2}$$

As the polar activity of a surface increases the contact angle of water will decrease. In this work, a w/o system is demonstrated in which a membrane shows selective permeability to oil and rejection of water. The above equation dictates how it is possible to design a membrane that can achieve the opposite result of complete rejection of oil droplets in an o/w system. Apart from this nuance in surface chemistry of the membrane, the principles and results of this study hold equally true for both w/o and o/w systems.

4.2 Wetting of Three Phase Systems

4.3 Breakthrough Pressure Model

Figure 4.1 demonstrates a steel mesh with openings 80 μm in size that can easily separate a stratified mixture of hexadecane and water. For small droplets however, the mesh is

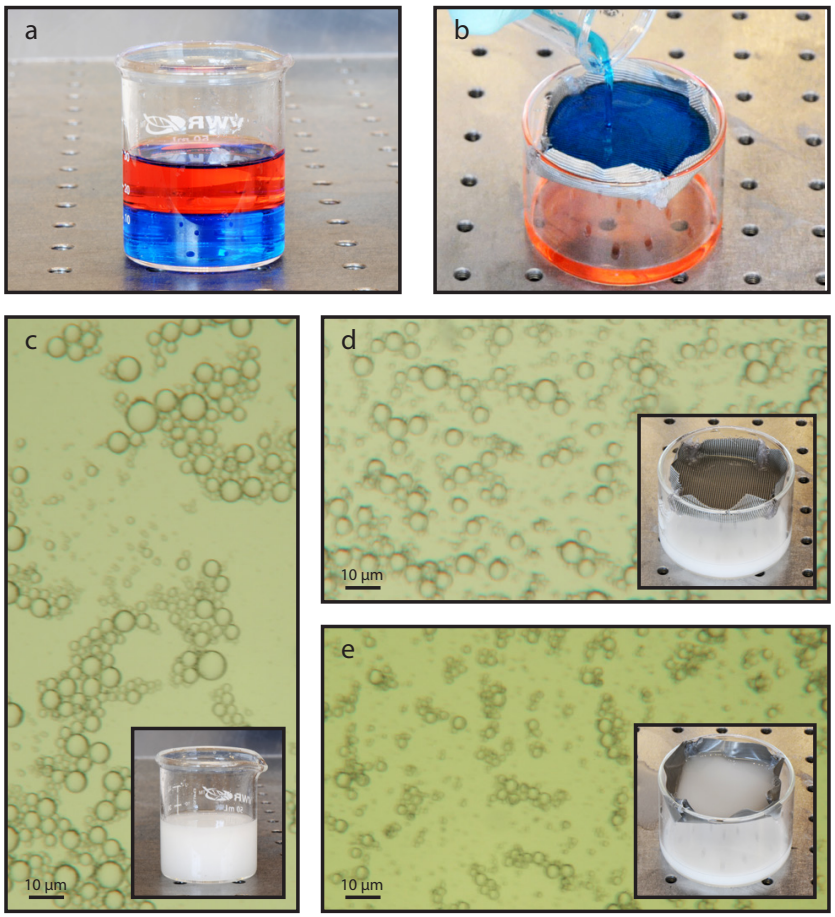

Figure 4.1: A stratified mixture of hexadecane (red) and water (blue) **a,** before pouring and **b,** after pouring through an 80 μm OTS coated mesh. Microscopic and macroscopic images of a 10 wt% w/o emulsion stabilized by Span 80 **c**, before filtration, **d**, filtered through an 80 μm OTS coated mesh and **e**, filtered through a 10 μm OTS coated mesh.

ineffective. If the mesh size is decreased to 10 μm, it is evident that droplets larger than the mesh size can be blocked but those smaller still pass through. To completely separate such emulsions, smaller pore sizes must be used in which it is necessary to supply a transmembrane pressure in addition to the hydrostatic head. Accordingly, it is important to understand another limitation on the system and introduce the concept of breakthrough pressure.

A membrane that can completely reject a dispersed phase takes advantage of the difference in surface energies between the two phases. Provided the droplet radius is larger than the pore diameter, a droplet will breakthrough the membrane at pressures exceeding the

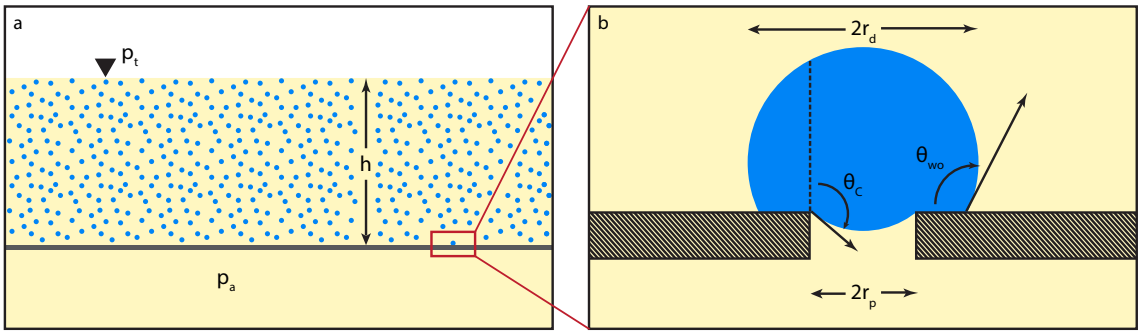

Figure 4.2: **a,** Model of a w/o emulsion being filtered through a membrane. **b,** Close-up diagram of a rejected droplet on the surface of the membrane.

breakthrough pressure which follows from the Young- Laplace equation. The schematic for this is shown in Figure 4.2.

$$P_B = \frac{2\gamma_{WO}\cos\theta_C}{r_p} \tag{4.3}$$

In order to achieve maximum rejection of water droplets, the transmembrane pressure P_t must be kept below the breakthrough pressure. Here the contact angle is taken to be the advancing contact angle of a water droplet on the substrate in a background of oil. Such an angle characterizes the largest angle that can be sustained before the contact line advances into the pore. Also, note that the relevant interface here is the interface between oil and water. In the design of this system, the membrane was more wetting to oil than water to achieve permeation of the oil phase.

Accordingly, there is a maximum achievable flowrate for all membranes filtering deformable media. If the driving pressure is high enough, the transmembrane pressure will exceed the breakthrough pressure and even large droplets will breakthrough the membrane.

In general, consider two immisible phases 1 and 2. Two necessary conditions must hold true for completed rejection of phase 2 and permeation of phase 1. First, the minimum droplet size of phase 2 must be larger than the maximum pore size of the membrane. Second, phase 1 must wet the membrane more than phase 2. In general, this can be ex-

pressed in the equations below.

$$r_{2,min} > r_{pore,max} \tag{4.4}$$

$$2(\sqrt{\gamma_S^{LW}\gamma_1^{LW}} + \sqrt{\gamma_S^{+}\gamma_1^{-}} + \sqrt{\gamma_S^{-}\gamma_1^{+}}) > 2(\sqrt{\gamma_S^{LW}\gamma_2^{LW}} + \sqrt{\gamma_S^{+}\gamma_2^{-}} + \sqrt{\gamma_S^{-}\gamma_2^{+}}) \tag{4.5}$$

The first equation represents the geometrical constraint while the second equation represents the energy requirements of the membrane. It incorporates polar components which can be tweaked to achieve a membrane that is more wetting to water than oil.

The presence of surfactants further complicates operation of such a system. In general, surfactants will vary the surface energy parameters. Other surface active compounds may adsorb to interfaces, and the resulting viscous interfacial films provide an additional mechanism that prevents droplet breakthrough. Due to the complexities that arise in systems comprising multiple types of surface active compounds, this study does not consider the effect of viscous interfacial films.

Figure 4.3 shows a simple acrylic filtration cell used to visualize the phenomenon of droplet breakthrough. The cell was constructed so that a pressure can be applied to control the transmembrane pressure. This cell was used both for filtration experiments presented later as well as visualization experiments.

In Figure 4.4, the filtration cell was filled with n-hexadecane. Dyed water droplets were then placed on the surface of a 600 nm OTS treated polycarbonate membrane. The chamber was then pressurized. The oil began flowing through the membrane, but the water droplets remained on the surface. As soon as the pressure was increased above the calculated breakthrough pressure of 25 psi, droplets began to penetrate the membrane as dictated by Equation 4.3. While this visualization used macroscopic droplets, the same principle holds for droplets much smaller.

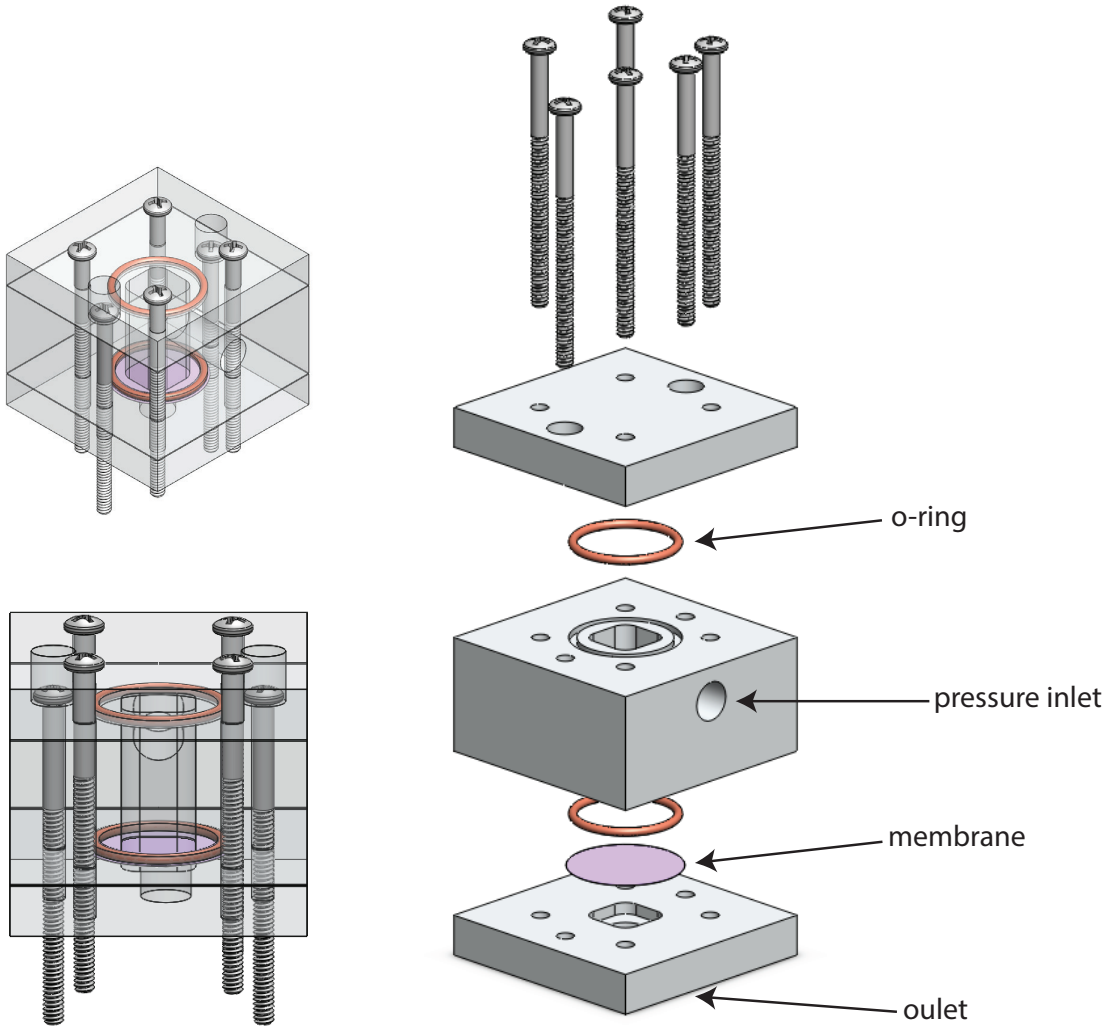

Figure 4.3: Model of the acrylic filtration cell used for filtration experiments and visualization studies. A pressure is applied via an inlet and permeate is collected through the bottom outlet. O-rings seal the chamber.

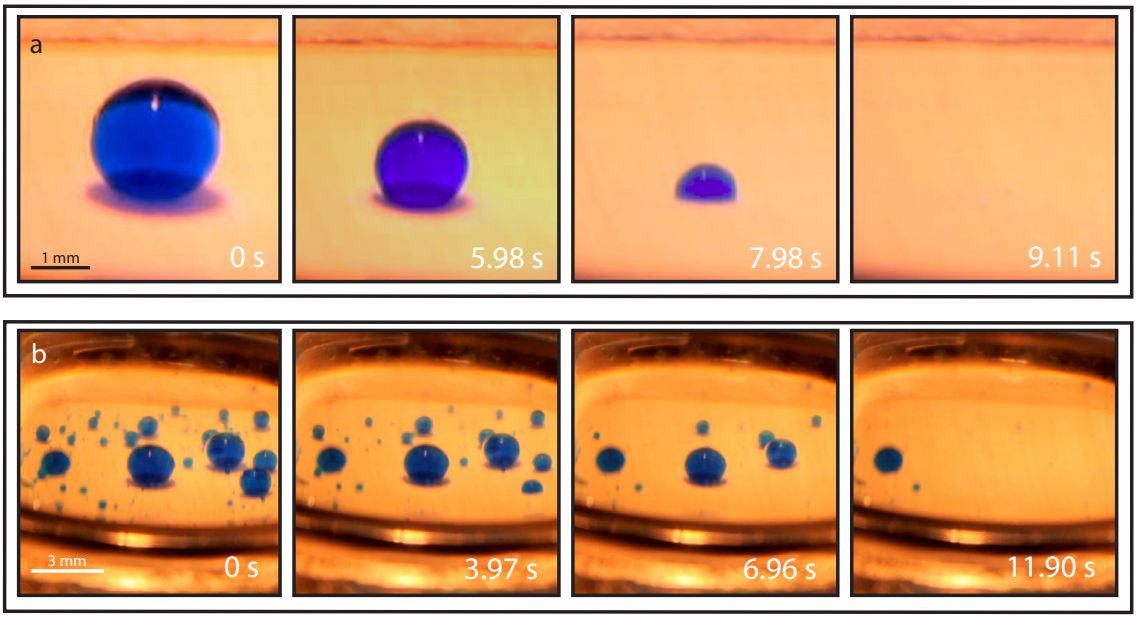

Figure 4.4: **a,** Frames from a video showing a 2 mm diameter droplet breaking through a 600 nm OTS coated polycarbonate membrane after the transmembrane pressure exceeds 25 psi. **b,** Frames from a video showing droplets of many sizes breaking through a 600 nm OTS coated polycarbonate membrane after the transmembrane pressure exceeds 25 psi. Note that the seemingly remaining droplet in the last frame is actual a droplet stuck to the side of the filtration cell and not in contact with the membrane.

4.4 Fabrication

To demonstrate the operation of membranes capable of filtering w/o emulsions, two polycarbonate membranes of pore sizes 600 nm and 100 nm were coated with octadecyltrichlorosilane (OTS, Sigma-Aldrich). The polycarbonate membranes (EMD Millipore) were manufactured by the track-etch method wherein polymer films undergo to ion bombardment followed by a chemical etch.[44] The pores sizes are very tightly distributed around the reported values and thus are useful for this controlled study.

OTS is an organometallic chemical comprising a long oleophilic carbon chain and a chlorosilane group and depicted in Figure 4.5. The chlorosilane groups react with water to form silanol groups that then react with hydroxyl groups on the polymer surface with by the elimination of water.[45] OTS increases the oleophilicity of the membrane surface while also increasing its hydrophobicity. This effectively increases the membrane breakthrough pressure by increasing the advancing contact angle of water on the membrane in a background of oil.

Typically, a solution of about 0.5 wt% OTS in toluene is used to dip-coat a substrate. Because many polymers readily dissolve in toluene, hexadecane was instead employed as the solvent. A 0.5 wt% OTS in hexadecane solution was used to coat the membranes. After the membrane was submerged, a 0.25 wt% water in ethanol solution was added to complete the reaction.

Both a top view and a cross-section view of the OTS coated 600 nm polycarbonate membrane are shown in Figure 4.6. The coating is only a few nanometers thick and thus does not significantly change the geometry of the membrane.

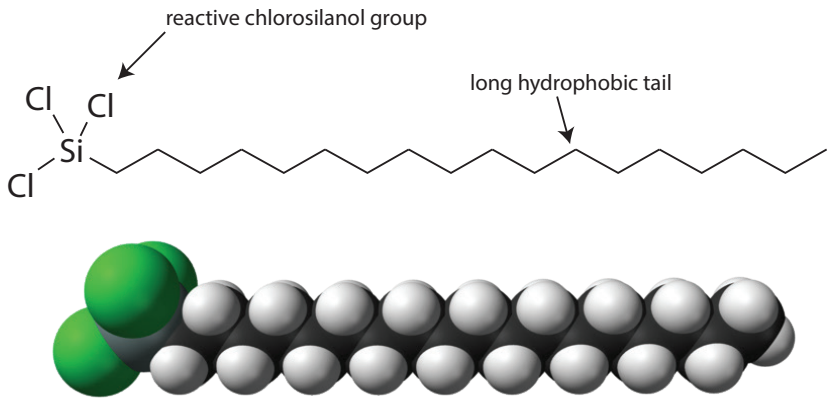

Figure 4.5: Schematic of the molecular structure of octadecyltrichlorosilane (OTS).

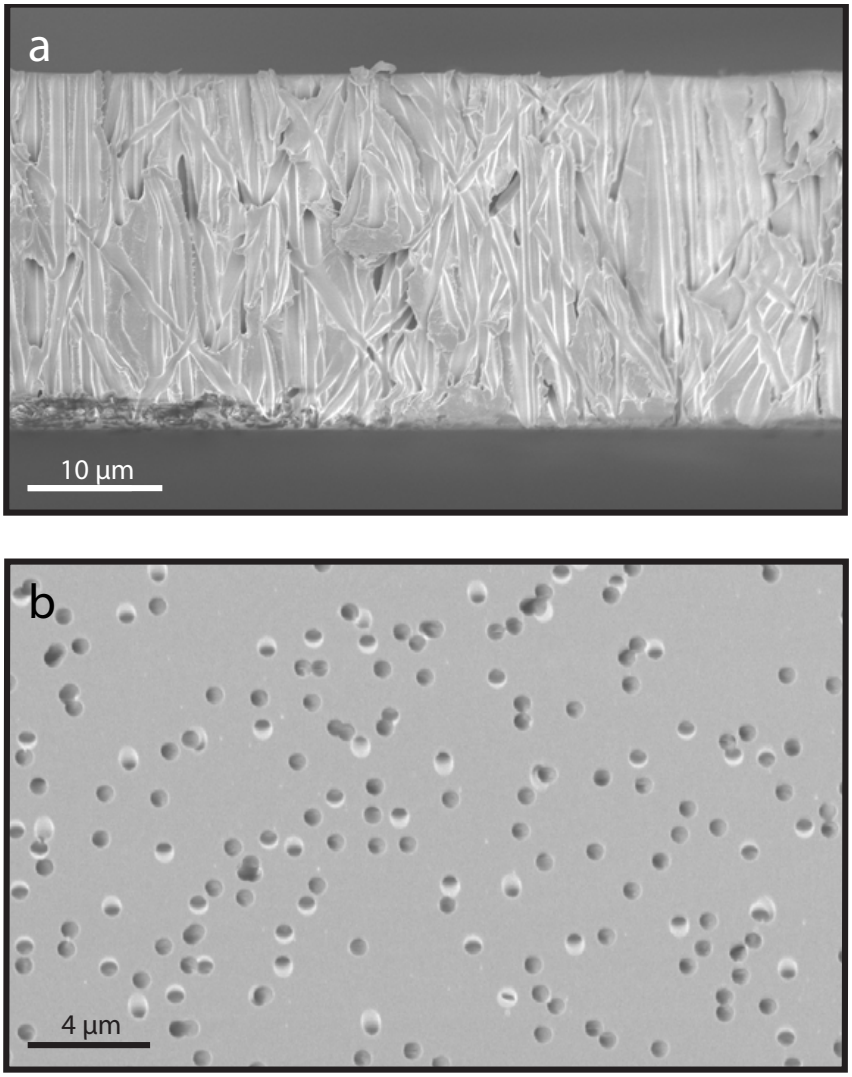

Figure 4.6: SEM images of an OTS coated 600 nm polycarbonate membrane showing the **e,** coated top side and **f,** cross section.

4.5 Experimental Methods

4.6 Results and Discussion

To demonstrate the filtration of extremely small droplets, the 100 nm membrane was tested by flowing a feed emulsion at a transmembrane pressure below the calculated breakthrough pressure. The feed emulsion was prepared by ultrasonication of a continuous phase of n-hexadecane with 1 wt% Span 80 non-ionic surfactant and 3 wt% water. Prior to filtration, the feed emulsion appears cloudy to the naked eye. Droplets of mean size around 1.5 μm can be seen by optical microscopy, and dynamic light scattering (DLS) shows much smaller droplets around 200 nm in diameter also present.

Passing the feed emulsion through the 100 nm membrane yields a visually clear permeate. Microscopy shows no evidence of droplets that were otherwise evident in the feed emulsion. DLS reveals that the smaller 200 nm droplets are non-existent in the permeate. Instead, a species of diameter around 10 nm is seen. It is hypothesized that these can be miscellar formations of Span 80 as this data peak was also seen in a solution of n-hexadecane contatining only 1 wt% Span 80 and no water. Interestingly, the membrane displayed a transient operation where the permeate at first was cloudy. In steady state however, the permeate was clear.

Differential scanning calorimetry (DSC) was used to probe the water content in the permeate samples. Samples were frozen to -20°C. Samples were then thawed at a rate of 2.4°C s^{-1}. The heat flow into the sample is measured. The crystalized water phase will melt around its melting points at 0°C and hexadecane around 18°C. Such a disparity in melting points allows the data to resolve into separate peaks for the water and hexadecane phases. Figure 4.7 shows the process for an emulsions containing 3 wt% water in 97 wt% hexadecane. When the water melts, a peak proportional to the mass of water appears. Similarly, when the hexadecane melts another peak is visible.

$$\Delta H_C = \int \frac{\mathrm{d}q}{\mathrm{d}t}\mathrm{d}t \tag{4.6}$$

The feed emulsions shows a noticeable peak at 0°C indicating the presence of water.

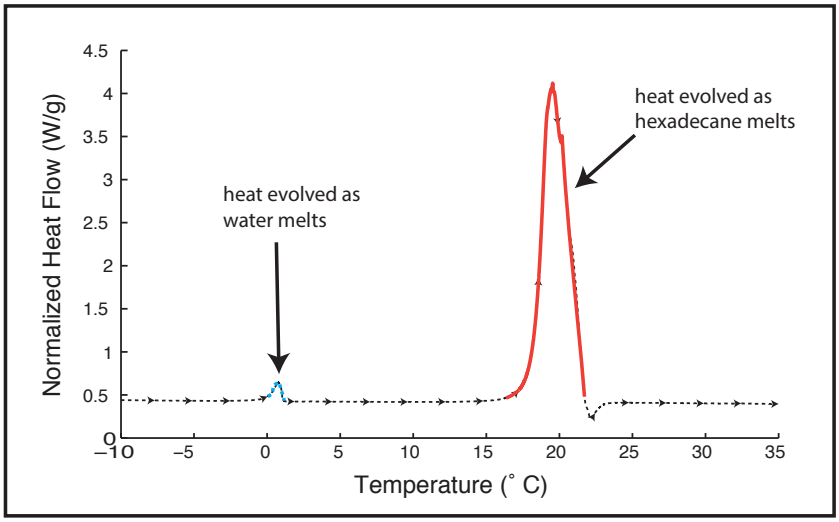

Figure 4.7: DSC data for a 3 wt% w/o emulsion demonstrating the relevant peaks.

This peak isnt present in the permeate sample, indicating the permeate has very low water content.

Figure 4.8 summarizes the results of the experiment. The feed emulsion passed through the membrane and resulted in a clear permeate. The permeate is free of water as judged by microscopy images, DLS data and DSC data.

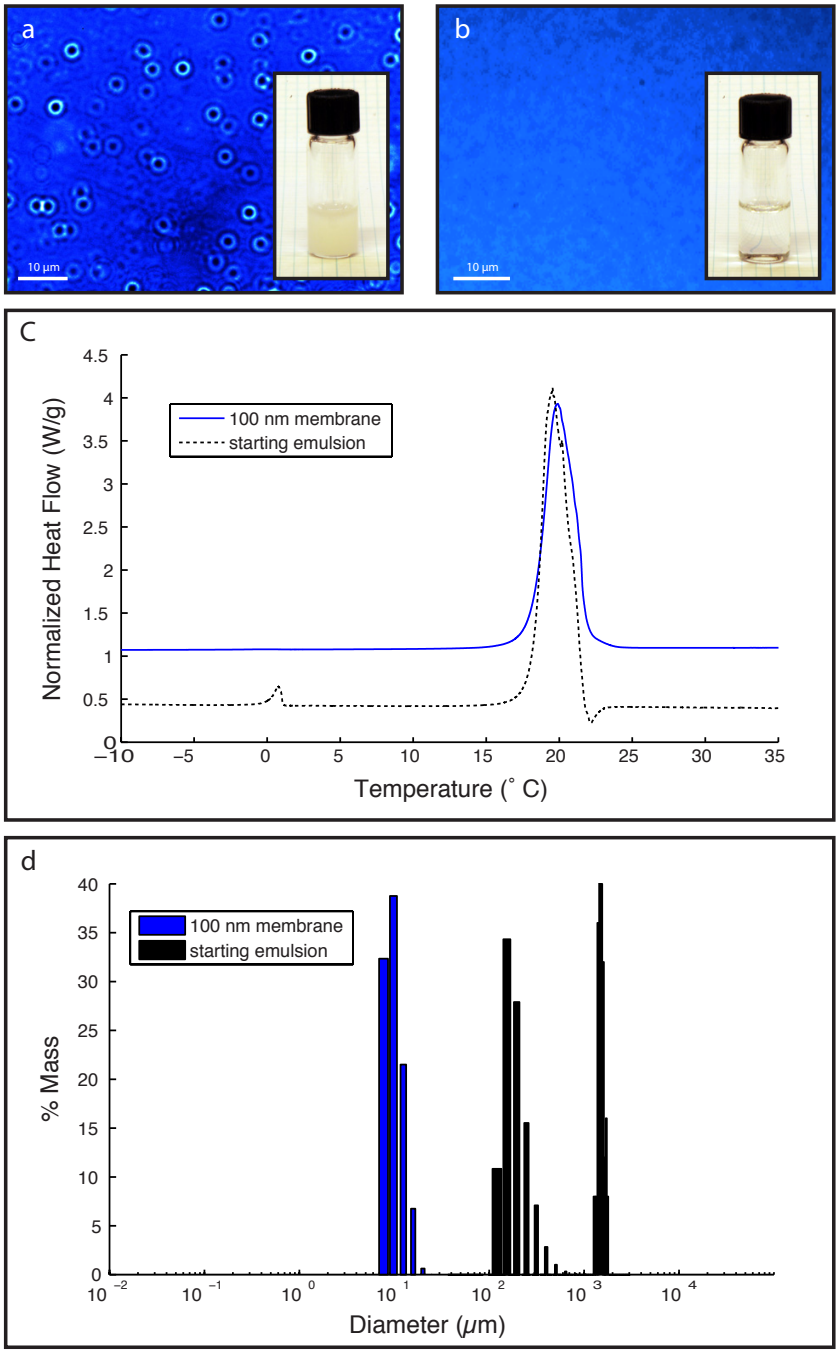

Figure 4.8: Microscopic and macroscopic photos of a 3 wt% w/o emulsions stabilized by Span 80 **a,** before filtration and **b,** filtered through a 100 nm OTS coated PC membrane at a transmembrane pressure below the breakthrough pressure. **c,** DSC data for the emulsion before filtration (black) and filtered through a 100 nm OTS coated PC membrane (blue). **d,** Distribution of droplets in the pre-filtered emulsion and permeate.

Chapter 5

Hierarchical Membranes for Improved Permeabilities

5.1 Design Philosophy

The commercial viably of track-etch membranes is limited because of their high cost. Although the chemical etching process involved in their manufacture scales well, the process of ion bombardment is difficult to achieve on large scales. In addition, so-called through-pore membranes in which the diameter of a pore is constant across the membrane thickness suffer an inherent tradeoff. As shown, the breakthrough pressure scales with the inverse of the pore size. Darcys Law is a phenomenologically derived constitutive equation that describes the flow of a fluid through a porous medium.

$$Q = \frac{-kA}{\mu}\frac{\Delta P}{L} \sim r^4 \tag{5.1}$$

Combining these two concepts, while small pores achieve higher breakthrough pressures, the flowrate for such geometries at such pressures rapidly decreases. In other words, through-pore geometries are confined to the following relation where p_p is the number pore density:

$$Q_{max} \sim \frac{\rho_p A \gamma_{WO} \cos\theta_C}{\mu}\frac{r^3}{L} \tag{5.2}$$

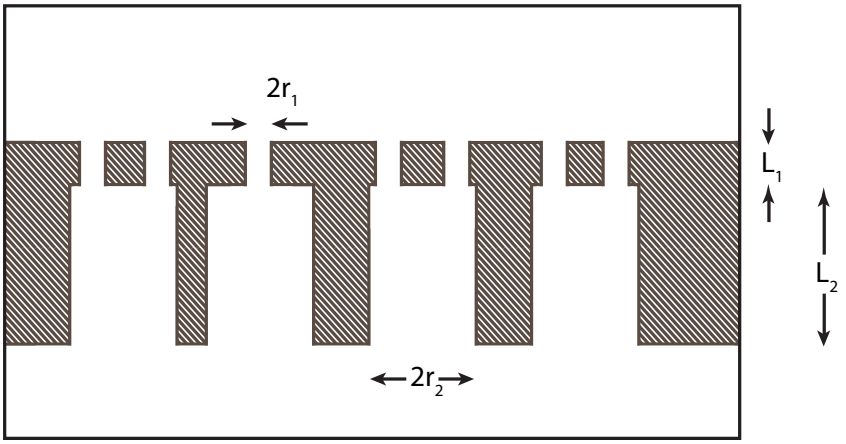

Figure 5.1: Diagram of an asymmetric membrane featuring a thin layer of small pores and thick layer of larger pores. Not to scale.

Asymmetrical geometries offer the potential to overcome this limitation. Polysulfone (Psf) is a practical, already manufactured membrane material that has been readily employed in many industries.[11,46] Such commercially available membranes are an established platform that can perform efficient separate of o/w and w/o emulsions with further chemical modification. Leveraging such a hierarchical structure allows the maximum flowrate limit to be circumvented.

Consider a model hierarchical structure with two layers depicted in Figure 5.1. A thin layer 1 with small pores is used to reject small droplets while a thick layer 2 allows for less resistance while providing mechanical stability.

$$Q_{max} \sim \frac{\rho_p A \gamma_{WO} \cos\theta_C}{\mu} \frac{1}{r_1 L} \left(\frac{1}{\frac{L_1}{r_1^4} + \frac{L_2}{r_2^4}} \right) \tag{5.3}$$

As evident, as the thin layer because thin, for a given total thickness and minimum pore size a greater flowrate can be achieved. In practice, it is difficult to achieve such membrane parameters to make an appreciable difference on flowrate, but it is in principle possible. In this study, the thickness of the skin layer was significantly varied by more than a factor of two by employing use of a number of additives.

5.2 Synthesis

Porous polysulfone (Psf) membranes were prepared using the phase inversion technique based on non-solvent induced phase separation method.[47] From SEM micrographs, the Psf membrane contains pores of sizes ranging from 100 nm to 10 μm. The SEM micrographs are included in Figure 5.2.

In essence, the phase-inversion method is a casting method. Sheets approximately 4 in x 8 in were casted, but the process can be easily scaled up for manufacture. To demonstrate the effectiveness of these membranes, membranes were cut into 25 mm filters and treated with OTS.

In addition, Psf membranes were also prepared with 5 and 10 wt% PEG as additives to reduce the skin thickness layer. Controlled optimization of such additives holds promise to further decrease the skin layer thickness and customize the membrane for separation of emulsions of varying droplet size distributions. The results of this study are summarized in the table below.

Psf concentration	PEG concentration	Skin thickness (μm)
100%	0%	1.7
95%	5%	1.6
90%	10%	0.8

5.3 Results and Discussion

The same 3 wt% w/o emulsion used for testing the polycarbonate membrane was filtered and the permeate was analyzed. The results are summarized in Figure 5.2. It performed similarly to the track-etched polycarbonate membrane and yielded a visually clear permeate. Microscopy shows no evidence of droplets that were otherwise evident in the feed emulsion. DLS reveals that the smaller 200 nm droplets are non-existent in the permeate. In addition, DSC did not show any trace of water in the permeate.

Preliminary results indicate that Psf membranes with thinner skin layers show improved permeability. However, the acrylic filtration chamber does not allow for precise enough

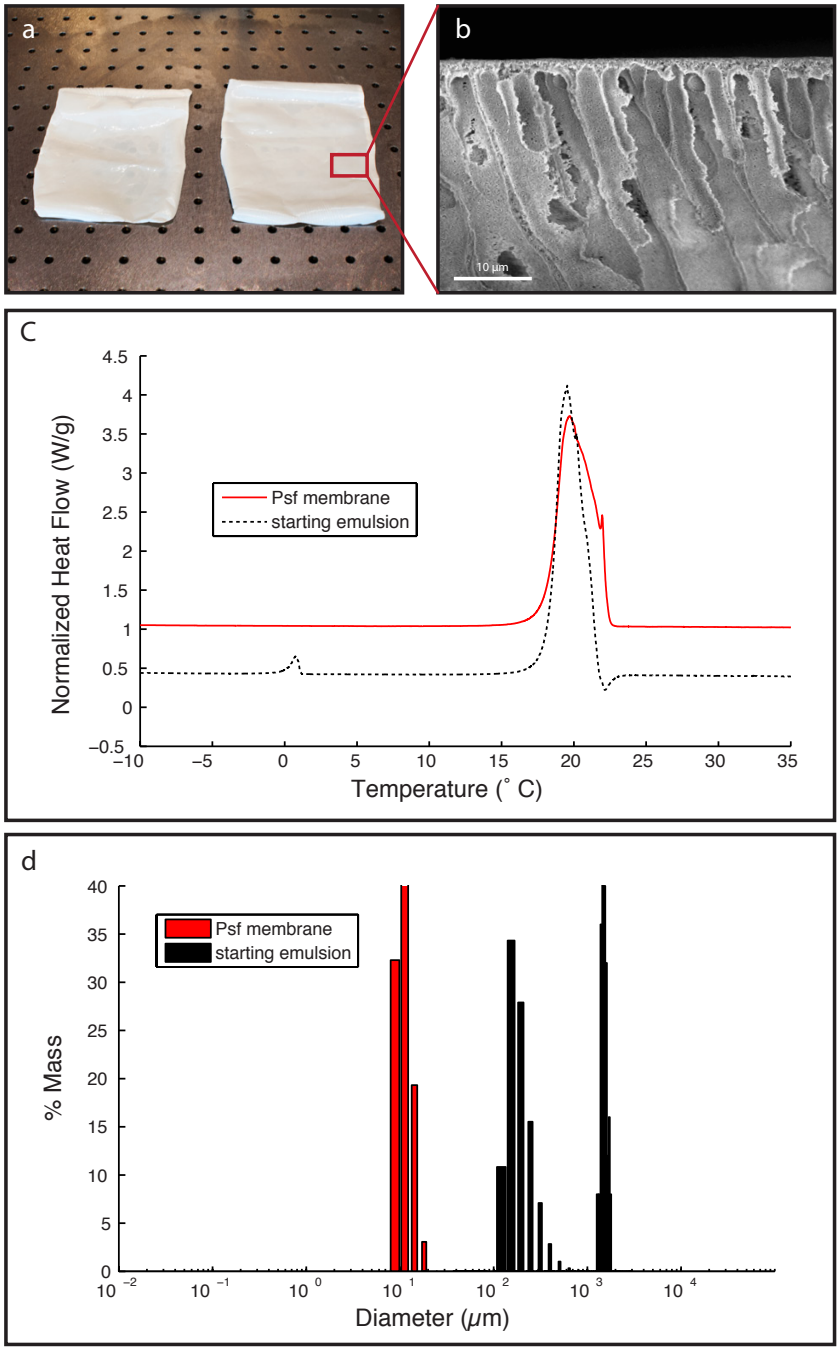

Figure 5.2: **a,** Photos of cast Psf membranes. **b,** SEM of the cross section of a Psf membrane showing asymmetric geometry featuring a skin layer. **c,** DSC data for the 3 wt% water-in-oil emulsion before filtration and filtered through the OTS coated Psf membrane. **d,** Distribution of droplets in the pre-filtered emulsion and permeate.

permeability measurements. Because the error is so large, conclusive results demonstrating improved permeabilities is still ongoing and will likely require a different system to test the

membranes.

Chapter 6

Conclusions and Recommendations

To conclude, the focus of this thesis was the design and testing of membranes for separation of a water-in-oil (w/o) emulsion. A polycarbonate membrane treated with octadecyltrichlorosilane (OTS) was used to filter a 3 wt% w/o emulsion. The permeate is characterized to have no measurable water content by microscopy, dynamic light scattering (DLS) and differential scanning calorimetry (DSC). To improve upon these results, a method for fabricating an asymmetric polysulfone membrane is presented. The polysulfone membrane has the feature of allowing much higher flow rates for a given applied pressure. The permeate of the Psf membrane also has no measurable water content.

The research is largely motivated by a need for low cost methods for separating o/w and w/o emulsions. The largest source of wastewater is generated by the petroleum industry as o/w emulsions. Currently, industry has a number of methods for cleaning produced water. The inherent problem is that the smaller dispersed droplets are the more they are to separate. The membrane technologies presented henceforth offer a new alternative.

In the future, the costs of this system must be better understood to determine whether the system is feasible for large scale produced water filtration. In addition, work characterizing the permeably of the assymteric polysulfone membranes is forthcoming. Preliminary results indicate that limited flow rates can indeed be circumvented by this novel design.

References

[1] R. Pfeifer, *GNU Free Documentation License* (2004).

[2] J. Shu, B. Grandjean, A. v. Neste, S. Kaliaguine, *The Canadian Journal of Chemical Engineering* **69**, 1036 (1991).

[3] C. Charcosset, *Journal of Chemical Technology and Biotechnology* **71**, 95 (1998).

[4] P. Bernardo, E. Drioli, G. Golemme, *Industrial & Engineering Chemistry Research* **48**, 4638 (2009).

[5] C. Neinhuis, W. Barthlott, *Annals of Botany* **79**, 667 (1997).

[6] J. D. Smith, *et al.*, *Soft Matter* **9**, 1772 (2013).

[7] H. Lee, M. L. Alcaraz, M. F. Rubner, R. E. Cohen, *ACS Nano* (2013).

[8] S. Nishimoto, B. Bhushan, *RSC Advances* **3**, 671 (2013).

[9] W. Reilly, T. OFarrell, M. Rubin, *US Environmental Protection Agency* (1991).

[10] C. W. Act, *Section* **404**, 40 (33).

[11] B. Chakrabarty, A. Ghoshal, M. Purkait, *Journal of Membrane Science* **325**, 427 (2008).

[12] J. Coca, G. Gutiérrez, J. Benito, *Water Purification and Management* (Springer, 2011), pp. 1–55.

[13] L. Xia, S. Lu, G. Cao, *Journal of Colloid and Interface Science* **271**, 504 (2004).

[14] J. D. McLean, P. K. Kilpatrick, *Journal of Colloid and Interface Science* **189**, 242 (1997).

[15] J. S. Eow, M. Ghadiri, *Chemical Engineering Journal* **85**, 357 (2002).

[16] M. Stewart, K. Arnold, *Emulsions and Oil Treating Equipment: Selection, Sizing and Troubleshooting* (Gulf Professional Publishing, 2008).

[17] W. L. McCabe, J. C. Smith, P. Harriott, *Unit Operations of Chemical Engineerings*, vol. 3 (McGraw-Hill Book Company New York, 1956).

[18] J. Maybury, K. Mannweiler, N. Titchener-Hooker, M. Hoare, P. Dunnill, *Bioprocess Engineering* **18**, 191 (1998).

[19] E. Vrablik, *Proceedings of Purdue Industrial Waste Conference* (1959), vol. 14.

[20] G. F. Bennett, R. W. Peters, *Critical Reviews in Environmental Science and Technology* **18**, 189 (1988).

[21] F. Rozada, L. Calvo, A. Garcı a, J. Martı n Villacorta, M. Otero, *Bioresource Technology* **87**, 221 (2003).

[22] J. W. Bush, D. L. Hu, *Annu. Rev. Fluid Mech.* **38**, 339 (2006).

[23] E. Villermaux, B. Bossa, *Nature Physics* **5**, 697 (2009).

[24] J. T. Davies, E. K. Rideal (1961).

[25] P. C. Hiemenz, R. Rajagopalan, *Principles of Colloid and Surface Chemistry, revised and expanded*, vol. 14 (CRC Press, 1997).

[26] A. T. Paxson, K. K. Varanasi, *Nature Communications* **4**, 1492 (2013).

[27] M. Ali, M. Alqam, *Fuel* **79**, 1309 (2000).

[28] R. Mohammed, A. Bailey, P. Luckham, S. Taylor, *Colloids and Surfaces A: Physicochemical and Engineering Aspects* **80**, 237 (1993).

[29] D. Thompson, A. Taylor, D. Graham, *Colloids and Surfaces* **15**, 175 (1985).

[30] E. Vignati, R. Piazza, T. P. Lockhart, *Langmuir* **19**, 6650 (2003).

[31] W. R. Bowen, F. Jenner, *Advances in Colloid and Interface Science* **56**, 141 (1995).

[32] N. Ochoa, M. Masuelli, J. Marchese, *Journal of membrane science* **226**, 203 (2003).

[33] S. P. Nunes, M. L. Sfora, K.-V. Peinemann, *Journal of Membrane Science* **106**, 49 (1995).

[34] L. F. Hancock, S. M. Fagan, M. S. Ziolo, *Biomaterials* **21**, 725 (2000).

[35] R. H. Davis, A. Z. Zinchenko, *Journal of Colloid and Interface Science* **334**, 113 (2009).

[36] S. Cobos, M. Carvalho, V. Alvarado, *International Journal of Multiphase Flow* **35**, 507 (2009).

[37] A. K. Kota, G. Kwon, W. Choi, J. M. Mabry, A. Tuteja, *Nature Communications* **3**, 1025 (2012).

[38] Z. Xue, *et al.*, *Advanced Materials* **23**, 4270 (2011).

[39] J. A. Howarter, J. P. Youngblood, *Journal of Colloid and Interface Science* **329**, 127 (2009).

[40] R. J. Good, *Journal of Adhesion Science and Technology* **6**, 1269 (1992).

[41] J. A. Howarter, K. L. Genson, J. P. Youngblood, *ACS Applied Materials & Interfaces* **3**, 2022 (2011).

[42] S. Turri, R. Valsecchi, M. Viganò, M. Levi, *Polymer Bulletin* **63**, 235 (2009).

[43] W. Wu, R. J. Giese, C. Van Oss, *Langmuir* **11**, 379 (1995).

[44] R. L. Fleischer, P. B. Price, R. M. Walker, *Nuclear tracks in solids: principles and applications* (Univ of California Press, 1975).

[45] T. M. Mayer, M. P. de Boer, N. D. Shinn, P. J. Clews, T. A. Michalske, *Journal of Vacuum Science & Technology B: Microelectronics and Nanometer Structures* **18**, 2433 (2000).

[46] A. Rezvanpour, R. Roostaazad, M. Hesampour, M. Nyström, C. Ghotbi, *Journal of Hazardous Materials* **161**, 1216 (2009).

[47] M. Hyder, R. Huang, P. Chen, *Journal of Membrane Science* **318**, 387 (2008).